Journal of Inflammation Research

Dovepress
Taylor & Francis Group

Open Access Full Text Article

ORIGINAL RESEARCH

MFG-E8 in Kawasaki Disease: Role in Endothelial Injury and Diagnostic Potential

Qiongfei Pei[1–3], Jing Zhang[1–3], Mengling Li[1–3], Penghui Yang[1–3], Fengchuan Jing[1–3], Qijian Yi[1–3]

[1]Department of Cardiovascular Medicine, Children's Hospital of Chongqing Medical University, National Clinical Research Center for Child Health and Disorders, Ministry of Education Key Laboratory of Child Development and Disorders, Chongqing, People's Republic of China; [2]Chongqing Key Laboratory of Pediatric Metabolism and Inflammatory Diseases, Chongqing, People's Republic of China; [3]National Clinical Key Cardiovascular Specialty, Key Laboratory of Children's Important Organ Development and Diseases of Chongqing Municipal Health Commission, Chongqing, People's Republic of China

Correspondence: Qijian Yi, Department of Cardiovascular Medicine, Children's Hospital of Chongqing Medical University, Chongqing, 400014, People's Republic of China, Tel/Fax +86 02363624344, Email qjyi2003@hotmail.com

Background: Kawasaki disease (KD) is a systemic vasculitis predominantly affecting children under five years old, with coronary artery lesions (CALs) being a severe complication. Despite the effectiveness of intravenous immunoglobulin (IVIG) therapy, a subset of patients remains unresponsive, necessitating alternative strategies. Milk Fat Globule Epidermal Growth Factor 8 (MFG-E8) is a secreted glycoprotein that functions as a bridge between damaged cells and phagocytes, conferring the ability to regulate immunity and inflammation. This study aimed to investigate the potential role of MFG-E8 in KD pathogenesis.

Methods: Serum levels of MFG-E8 were measured via ELISA. CAWS was utilized to induce a murine model of coronary vasculitis, with MFG-E8 being administered intraperitoneally for treatment. Histological evaluation was conducted using H&E and IHC staining. Serum-stimulated THP-1 cells were co-cultured with endothelial cells to establish an inflammatory environment in vitro, with exogenous supplementation of MFG-E8. Pyroptosis-related markers were assessed by Western blot or immunofluorescence staining. Oxidative stress-related indicators were measured using commercially available assay kits.

Results: Serum MFG-E8 levels were significantly lower in KD patients, especially those with CALs, compared to febrile and healthy controls. ROC analysis showed that combining MFG-E8 with Fbg and TT improved the ability to distinguish KD from other febrile illnesses. Further analyses displayed negative correlations between MFG-E8 and parameters pointing to inflammation. In the murine model of vasculitis, MFG-E8 supplementation alleviated coronary artery inflammation, reduced endothelial cell pyroptosis, and mitigated oxidative stress. Similar results were presented in vitro experiments using KD serum-treated endothelial cells.

Conclusion: MFG-E8 represents a potential biomarker for the diagnosis of KD and exhibits protective effects against endothelial cell injury during the acute phase.

Keywords: Kawasaki disease, MFG-E8, endothelial cell pyroptosis, oxidative stress, coronary artery lesions

Background

Kawasaki disease (KD), also known as mucocutaneous lymphnode syndrome (MCLS), is most common in infants and children under 5 years old[1] and is characterized by systemic vasculitis involving small and medium-sized arteries, especially the coronary arteries.[2] Previous data have revealed that 20–25% of untreated children with Kawasaki disease will suffer from coronary artery lesions (CALs).[3,4] With the damage persisting or progressing, more serious cardiovascular events such as myocardial infarction or sudden death occur,[5] making KD a leading cause of pediatric-acquired heart disease in developed countries.[6] Timely and standardized intravenous immunoglobulin (IVIG) therapy is considered the mainstay of treatment in the acute phase of KD[7] and can significantly reduce the incidence of coronary artery aneurysms (CAA).[8] Therefore, early and accurate identification of KD is crucial for its prognosis. However, given that the early detection of most KD cases is largely dependent on clinical manifestations, incomplete KD and other febrile diseases with similar presentations add challenges to clinical decision-making.[9,10] Appropriate biomarkers will be instrumental in achieving early diagnosis and treatment of KD.

Received: 17 June 2025
Accepted: 15 November 2025
Published: 21 November 2025

Although immunity and inflammation are thought to be two core links in the KD process[11,12] and a large body of research has been carried out accordingly, it is still difficult to be conclusive about its pathogenesis. Especially regarding coronary artery lesions, a number of patients have demonstrated non-response to IVIG treatment.[13,14] Other supplementary approaches, including a second round of IVIG, glucocorticoid steroids, infliximab, etc., have lacked evidence of a significant reduction in the incidence of CAA.[15] Hence, more potential therapeutic directions need to be explored to acquire better clinical outcomes.

Pyroptosis is a form of programmed cell death closely related to inflammatory responses and is involved in multiple organs and various diseases.[16] Recently, its increasing prominence in the cardiovascular field has also been noted,[17] with the participation of a wide range of cells including endothelial cells, cardiomyocytes, macrophages, neutrophils, and peripheral blood mononuclear cells (PBMCs). Several studies have focused on the relationship between pyroptosis and KD, emphasizing that the activation of NOD-like receptor thermal protein domain associated protein 3 (NLRP3) inflammasome and the release of its downstream products are crucial in the immunopathology of KD.[18,19] Among them, endothelial cell pyroptosis mediated by the HMGB1/RAGE signaling pathway plays an important role in Candida albicans cell wall extracts (CAWS)-induced vasculitis,[20] suggesting new possibilities for therapeutic targets in KD.

Milk fat globule epidermal growth factor (EGF) factor 8 (MFG-E8), also known as lactadherin, is a secreted lipophilic glycoprotein. It contains a highly conserved arginine–glycine–aspartate (RGD) motif, by which avβ3/avβ5 integrin receptors of phagocytic cells are recognized, while the C-terminal factor V/VIII-like domains enable it to bind to the apoptotic cells via phosphatidylserine (PS).[21] Given this scavenger role, MFG-E8 has been proven a regulator in inflammation and autoimmune diseases.[22] Notably, quite a few studies are emerging in the cardiovascular field. In addition to promoting phenotypic switching of smooth muscle cells[23,24] and inhibiting endothelial-to-mesenchymal transition,[25] MFG-E8 can attenuate cardiac remodeling and adverse fibrosis secondary to acute myocardial infarction by accelerating the clearance of damaged cardiomyocytes.[26] Nevertheless, the relationship between MFG-E8 and KD has not yet been described. Analysis of a KD-associated set in the GEO database indicates that the mRNA expression of MFG-E8 in PBMCs of KD patients during the acute phase is significantly lower than that of healthy children (Figure S1), which is consistent with the changes that it presents in other inflammatory diseases. Hence, the current study was conducted to explore the reasons for the above phenomenon and to obtain a better understanding of the relationship between MFG-E8 and KD.

Methods

Subjects

All serum samples in this study were obtained from the Children's Hospital of Chongqing Medical University. The sample size was estimated based on our pre-experiments. Informed consent was obtained from parents or legal guardians and approval from the Ethics Committee of Children's Hospital of Chongqing Medical University was received for this study (approval no. 2023–586). All procedures were carried out following relevant guidelines and regulations addressed in the Declaration of Helsinki.

The diagnostic criteria for KD were implemented according to the guidelines proposed by the Japanese Circulation Society Joint Working Group. Exclusion criteria included: the combination of other autoimmune diseases; a previous history of KD; and treatments of IVIG outside our hospital during the current course of the disease. Diagnoses of febrile controls (FC) included pneumonia and sepsis. Normal controls (NC) come from the physical examination department.

Echocardiography was performed in KD patients before initial treatment. Z-scores of coronary arterial internal diameters were calculated on the basis of body surface area using the LMS method. Patients with Z-scores ≥ 2.0 were allocated into the KD patients with CALs (CALs) group, while those with Z-scores < 2.0 were allocated into the KD patients non-CALs (NCALs) group. All the cardiac ultrasound examinations were performed by expert physicians who were unblinded to the clinical information.

A total of 88 patients with KD (KD group), including 56 in the NCALs subgroup and 32 in the CALs subgroup, as well as 52 febrile controls (FC group) and 30 normal controls (NC group), were enrolled in this study from December 2023 to March 2024 consecutively.

Sample and Data Collection

Blood samples were collected before the initial IVIG treatment. Serum was isolated by centrifugation at 3000 rpm for 10 min and stored at −80°C for later use. The same procedure was followed to obtain serum from febrile and healthy children.

Laboratory parameters of KD and FC children were collected before the initial treatment, including prothrombin time (PT), activated partial thromboplastin time (APTT), fibrinogen (Fbg), thrombin time (TT), D-dimer (DD), creatine kinase-MB (CK-MB), white blood cell counts (WBC), lymphocyte count (LYM), neutrophilic granulocyte count (GRAN), monocyte count (MONO), percentage of lymphocytes (L%), percentage of neutrophils (N%), platelet counts (Plt), red blood cell counts (RBC), hematocrit (Hct), hemoglobin (Hb), procalcitonin (PCT), C-reactive protein (CRP), erythrocyte sedimentation rate (ESR), interleukin-2 (IL-2), interleukin-10 (IL-10), and interferon-gamma (IFN-γ).

Neutrophil-to-lymphocyte ratio (NLR) and platelet-to-lymphocyte ratio (PLR) were calculated as neutrophil and platelet counts divided by lymphocyte counts, respectively.

Enzyme-Linked Immunosorbent Assay

Serum levels of MFG-E8 were determined by the corresponding ELISA kits according to the manufacturer' s instructions. The ELISA kits for human and mouse MFG-E8 were purchased from BOSTER (Wuhan, China) and MEIMIAN (Jiangsu, China), respectively.

Preparation of CAWS

As previously reported,[27,28] the CAWS were prepared from Candida albicans strain NBRC1385. Briefly, C. albicans were cultivated in a C-limiting medium at 27°C for 2 days at a rotation speed of 270 rpm. Next, an equal volume of ethanol was added and thoroughly mixed, then kept at 4°C overnight. The cultures were collected by centrifugation, and the precipitate was dissolved in water for at least 2 hours. The complex was subsequently centrifuged again, obtained the supernatant was mixed with an equal volume of ethanol and left to stand at 4°C overnight. Finally, the precipitate acquired by centrifugation is subjected to drying. The prepared CAWS were dissolved in 0.9% normal saline and autoclaved before use.

Animals and Experimental Design

All experimental procedures were conducted in accordance with the Guide for the Care and Use of Laboratory Animals established by the Chongqing Science and Technology Commission and were approved by the Animal Ethics Committee of the Children's Hospital of Chongqing Medical University (approval no. CHCMU-IACUC20240628007). Male C57BL/6 mice at the age of 3–4 weeks were housed in a specific pathogen-free environment at the Animal Care Center of Children's Hospital of Chongqing Medical University. The mice were kept in a 12-hour light/dark cycle (7 am to 7 pm) with controlled temperature and humidity as well as free access to water and food. Prior to the initiation of the experiments, the mice underwent a 7-day acclimation period. For the observation of the model, the first cohort of mice were grouped according to different time points after CAWS induction (0, 3, 5, 7, and 14 days) and subjected to histological evaluation. The second cohort of mice were randomly divided into two groups (n=7 for each group): PBS group and CAWS group. For the assessment of MFG-E8 effects, mice were randomly divided into three groups (n=8 for each group): PBS group, CAWS group, CAWS+MFG-E8 group. Mice in the CAWS group were intraperitoneally (i.p.) injected daily with CAWS (4mg/body) dissolved in 0.2 mL of saline for 5 consecutive days, whereas mice in the PBS group received an equal volume of saline injection. Recombinant mouse MFG-E8 protein (R&D Systems, USA) (30 μg/kg) was intraperitoneally administered into mice every other day and 12 hours prior to CAWS induction. On day 14 of post-final CAWS induction, mice were anesthetized and sacrificed for the collection of appropriate specimens and follow-up examinations.

Hematoxylin and Eosin (H&E) Staining and Immunohistochemistry (IHC) Staining

The fixed heart tissues were embedded in paraffin and sectioned into 4 μm slices. Following dewaxing and hydration, the sections were then stained with H&E solution and observed under a light microscope. IHC staining was performed using a commercial kit (ZSGB-BIO, China). Briefly, slices subjected to antigen retrieval were incubated in 3% hydrogen peroxide solution at room temperature for 10 min to remove endogenous peroxidase, followed by blocking with goat

serum for 1 hour. The Ly6g primary antibody (1:2000, Servicebio) was used to stain neutrophils and incubated at 4°C overnight. Next, biotin-labeled goat anti-rabbit IgG and streptomycin-ovalbumin working solution labeled with horseradish peroxidase (HRP) were successively used for detection. Diamino benzidine was applied as a substrate for color development. Finally, sections were counterstained with hematoxylin.

Immunofluorescence Staining

Paraffin-embedded sections of heart tissue were deparaffinized through xylene, hydrated through graded alcohols, and immersed in appropriate solutions for antigen retrieval. Then, the sections were blocked with goat serum for 1 hour, followed by incubating with the anti-MFG-E8 antibody (1:100, Cat. No.: A12322, ABclonal), anti-SM22 antibody (1:100, Cat. No.: 60213-1-lg, Proteintech), anti-NLRP3 antibody (1:100, Cat. No.: 27458-1-AP, Proteintech), and anti-CD31 antibody (1:100, Cat. No.: M1511-8, HUABIO) at 4°C overnight. Then, the Alexa Fluor 647-labeled goat anti-mouse IgG (1:300, Cat. No.: A0473, Beyotime), FITC-labeled goat anti-rabbit IgG (1:300, Cat. No.: A0562, Beyotime), and Cy3-labeled goat anti-rabbit IgG (1:200, Cat. No.: GB21303, Servicebio) were applied at room temperature for 1 hour. Nuclei were stained by DAPI (C1005, Beyotime, China) for 10min. Images were captured under confocal laser microscopy (Nikon, Japan).

Real-Time Quantitative Polymerase Chain Reaction (RT-qPCR)

Total RNA was extracted from heart tissues using a commercial RNA extraction kit (AG21017, Accurate Biotechnology, China). RNA concentration and purity were determined using a NanoDrop 2000 spectrophotometer (NanoDrop Technologies, USA). First-strand complementary DNA (cDNA) synthesis was performed on 1 μg of RNA using an Evo M-MLV RT Mix Kit with gDNA Clean for qPCR Ver.2 (AG11728, Accurate Biotechnology, China). RT-qPCR was conducted to detect cDNA levels of vascular cell adhesion molecule-1 (VCAM-1) using the CFX Manager software detection system (Bio-Rad, USA). Primer sequences were as follows: VCAM-1 (forward: 5′- TTTCTGGGGCAGGAAGTTAGA, reverse: 5′- TCACAGCCAATAG CAGCACAC), β-actin (forward: 5′-CATCCGTAAAGACCTCTATGCCAAC, reverse: 5′- ATGGAGCCACCGATCCACA).

Western Blot (WB)

Heart tissues or endothelial cells were lysed on ice for 30 min using RIPA lysis buffer (P0013B, Beyotime, China), followed by centrifuging at 12,000 rpm for 10 min at 4°C. The supernatant containing total protein was quantified with BCA reagents. Proteins (40 μg/lane) were separated by sodium dodecylsulfate-polyacrylamide gel electrophoresis (SDS-PAGE) and electro-transferred onto polyvinylidene difluoride (PVDF) membranes (Millipore, USA). After blocking with 5% skimmed milk at room temperature for 2h, membranes were incubated with the following primary antibodies at 4°C overnight: NLRP3 (1:1000, Cat. No.: 15101S, Cell Signalling Technology), GSDMD (1:1000, Cat. No.: HA601046, HUABIO), cleaved N-terminal GSDMD (1:1000, Cat. No.: 36425S, Cell Signalling Technology; 1:1000, Cat. No.: ab219800, Abcam), β-actin (1:10,000, Cat. No.: EM21002, HUABIO; 1:50,000, Cat. No.: 250132, Zenbio). After washing with TBS containing 0.1% Tween-20, membranes were incubated with corresponding HRP-conjugated secondary antibodies at room temperature for 1 h. Bands were visualized by ChemiDoc™ MP Imaging System (Bio-Rad, USA). Relative protein expression was quantified using Image Lab software (Bio-Rad, USA) and normalized to β-actin.

Cell Culture and Treatments

EA.hy926 endothelial cells (ATCC CRL-2922, USA) were cultured in high-glucose Dulbecco's Modified Eagle Medium (DMEM) supplemented with 10% fetal bovine serum (FBS), and 1% penicillin/streptomycin at 37°C in a humidified atmosphere containing 5% CO2. THP-1 cells (ATCC TIB-202, USA) were transferred into cell culture flasks 75 cm2 and maintained in RPMI-1640 medium with 10% FBS and 1% penicillin/streptomycin. In the co-culture system, EA.hy926 cells were seeded in the lower chamber, while THP-1 cells were cultured in the upper chamber, allowing for the diffusion of soluble molecules. Then, KD or HC serum was added to the upper chamber and maintained in action for 24 hours. All cultures were grown in DMEM mediums. If appropriate, the recombinant human MFG-E8 protein (Abclonal, China) will be pre-incubated with endothelial cells 2 hours before stimulation.

TEM Examination

Abundant treated cells were collected and fixed in ice-cold 3% glutaraldehyde for 24 hours, followed by agarose pre-embedding, 1% osmium tetroxide post-fixing, ethanol gradient dehydration, epoxy resin embedding, polymerization, and staining. Finally, the sections were examined under a transmission electron microscope (TEM).

Detection of SOD, GSH-Px, and MDA Levels

The serum of mice and the homogenates of cells were obtained. Total Superoxide Dismutase Assay Kit with WST-8 (S0101S, Beyotime, China) and Cellular Glutathione Peroxidase Assay Kit with DTNB (S0057S, Beyotime, China) were used to determine the activity of superoxide dismutase (SOD) and glutathione peroxidase (GSH-px), respectively. Malondialdehyde assay kit (A003-1, Nanjing Jiancheng, China) was applied to assess the levels of malondialdehyde (MDA). All procedures were performed according to the manufacturer's instructions for the respective kits.

Cell Viability and LDH Release

An indirect co-culture model was adopted in such experiments. Briefly, THP-1 cells were maintained in the upper chambers and received serum stimulation. Next, the culture medium from the lower chambers was collected to treat endothelial cells that had been pre-incubated in 96-well plates. To obtain an optimal effect, a series of concentrations (0, 100, 200, 400, 600, 800, 1000ng/mL) of MFG-E8 was administered before treatment. Viability of EA.hy926 cells was detected by adding 10μL solution from Cell Counting Kit-8 (CCK8) Assay Kit (Dojindo, Japan) to the cells and incubating for 2 h at 37°C. The absorbance at 450nm was measured using a microplate reader (BioTek, USA). In addition, cell culture supernatants were collected and analyzed using a lactate dehydrogenase (LDH) cytotoxicity assay kit (Beyotime, China).

The absorbance at 490nm was obtained and the LDH release was calculated by dividing the positive well after subtracting the negative well.

Statistical Analysis

Statistical analyses were performed with GraphPad Prism 9 (GraphPad Software, San Diego, CA, USA). The normality of data was checked using the Shapiro–Wilk test. Continuous variables are presented as mean±standard deviation, or median (P25-P75). The Student's *t*-test was used for data simulated from a normal distribution, while the nonparametric Mann–Whitney *U*-test was selected for data that did not satisfy the normality assumption. One-way analysis of variance (ANOVA) was applied to multi-group comparisons. The Chi-square test was used for count data. Spearman's rank correlation was taken to analyze the correlation between serum MFGE8 levels and other laboratory parameters. Statistical significance was set at $p \leq 0.05$; ns, not significant; $^{*}p < 0.05$, $^{**}p < 0.01$, $^{***}p < 0.001$ and $^{****}p < 0.0001$; $^{\#}p < 0.05$.

Results

Serum MFG-E8 Levels and Laboratory Parameters in All Study Subjects

As shown in Figure 1A, the serum levels of MFG-E8 in the KD group [614.133 pg/mL (502.077, 796.785)] were significantly lower than those in the NC [776.261 pg/mL (635.877, 1022.86)] ($p = 0.005$) and FC [800.708 pg/mL (597.626, 1519.390)] ($p < 0.0001$) groups. Similarly, lower values were observed in the CALs group [551.482 pg/mL (466.676, 697.218)] compared with the NCALs group [694.522 pg/mL (514.344, 847.831)] ($p = 0.036$) (Figure 1B).

Regarding other laboratory parameters, without statistical differences in age and gender, the levels of PT, APTT, Fbg, DD, WBC, GRAN, N%, NLR, PCT, and CRP were significantly higher in the KD group compared to the FC group, while TT, CK-MB, L%, RBC, Hct, and Hb presented lower levels (Table 1).

Besides, no significant difference was found in PT, DD, CK-MB, WBC, MONO, L%, N%, Plt, RBC, Hb, PCT, IL-2, IL-10, and IFN-γ between the CALs and NCALs groups. APTT, Fbg, NLR, PLR, CRP, and ESR, however, tended to be higher in the CALs group. In contrast, TT, LYM, and Hct showed lower levels in this group (Table 2).

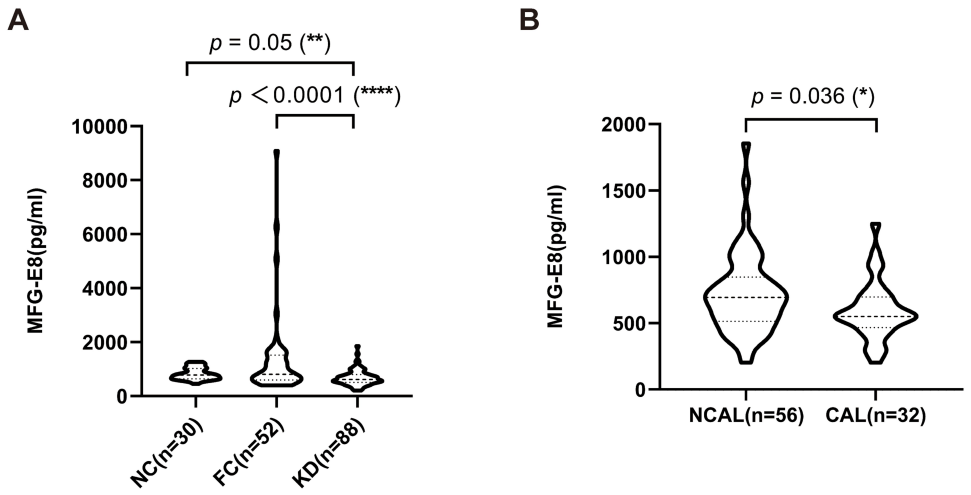

Figure 1 Serum MFG-E8 levels in all subjects. (**A**) The levels of MFG-E8 in NC, FC, and KD groups. (**B**) The levels of MFG-E8 in CALs and NCALs groups. Significance: *$p < 0.05$, **$p < 0.01$, ****$p < 0.0001$.

Diagnostic Performance of MFG-E8 for KD

The receiver operating characteristic (ROC) curves were analyzed individually for the indicators that demonstrated variability between the FC and KD groups. Fbg and TT were selected based on their favorable performances in the three primary evaluation

Table 1 General Clinical Parameters in the FC and KD Groups

Variable	FC (n=52)	KD (n=88)	*p* value
Age (mo)	31.000 (16.000, 50.750)	37.000 (20.000, 60.000)	0.101
Gender (male/female)	28/24	53/35	0.460
PT (s)	10.600 (10.225, 11.075)	12.300 (11.700, 13.300)	0.000****
APTT (s)	27.250 (25.175, 30.250)	30.500 (28.450, 33.000)	0.000****
Fbg (g/L)	3.960 (3.145, 4.600)	6.800 (5.470, 7.650)	0.000****
TT (s)	16.600 (15.925, 17.325)	14.800 (14.400, 15.400)	0.000****
DD (mg/L)	0.535 (0.340, 0.943)	1.555 (0.955, 2.473)	0.000****
CK-MB (ug/L)	1.080 (0.370, 1.850)	0.590 (0.240, 0.970)	0.002**
WBC (10^3/ul)	8.120 (6.103, 11.150)	14.130 (11.175, 16.810)	0.000****
LYM (10^3/ul)	2.895 (1.808, 4.658)	3.020 (2.320, 3.950)	0.957
L%	35.400 (25.300, 47.300)	22.000 (9.400, 28.600)	0.000****
GRAN (10^3/ul)	4.580 (2.515, 6.465)	8.920 (6.800,12.410)	0.000****
N%	55.600 (40.700, 65.100)	66.000 (45.500, 74.500)	0.046*
MONO (10^3/ul)	0.605 (0.335, 0.923)	0.565 (0.413, 0.765)	0.652
Plt (10^3/ul)	354.000 (262.000, 439.750)	344.000 (287.000,414.000)	0.605
RBC (10^6/ul)	4.440 (4.210, 4.650)	4.075 (3.865, 4.320)	0.000****
Hct (%)	36.150 (33.700, 37.875)	32.700 (30.900, 34.700)	0.000****
Hb (g/L)	118.500 (112.000, 125.750)	110.000 (103.000, 116.000)	0.000****
NLR (10^3/ul/10^3/ul)	1.547 (0.966, 2.657)	2.936 (2.053, 5.418)	0.000****
PLR (10^3/ul/10^3/ul)	121.102 (83.887, 151.717)	125.738 (92.405, 162.121)	0.586
PCT (ng/mL)	0.175 (0.093, 0.258)	0.410 (0.205, 1.330)	0.000****
CRP (mg/dl)	11.890 (1.555, 28.430)	59.000 (27.900, 99.000)	0.000****

Notes: *$p < 0.05$, **$p < 0.01$, ****$p < 0.0001$.

Abbreviations: FC, febrile controls; KD, Kawasaki disease; PT, prothrombin time; APTT, activated partial thromboplastin time; Fbg, fibrinogen; TT, thrombin time; DD, D-dimer; CK-MB, creatine kinase-MB; WBC, white blood cell counts; LYM, lymphocyte count; L%, percentage of lymphocytes; GRAN, neutrophilic granulocyte count; N%, percentage of neutrophils; MONO, monocyte count; Plt, platelet counts; RBC, red blood cell counts; Hct, hematocrit; Hb, hemoglobin; NLR, neutrophil-to-lymphocyte ratio; PLR, platelet-to-lymphocyte ratio; PCT, procalcitonin; CRP, C-reactive protein.

Table 2 General Clinical Parameters in the NCALs and CALs Groups

Variable	CALs (n=32)	NCALs (n=56)	*p* value
Age (mo)	43.000 (28.000, 68.500)	31.500 (20.000, 53.500)	0.097
Gender (male/female)	23/9	30/26	0.092
PT (s)	12.300 (12.025, 13.375)	12.200 (11.450, 12.950)	0.217
APTT (s)	31.100 (28.850, 34.200)	30.000 (28.400, 32.300)	0.024*
Fbg (g/L)	7.520 (6.453, 7.785)	6.150 (4.960, 7.590)	0.001**
TT (s)	14.700 (14.400, 14.975)	15.200 (14.500, 15.600)	0.044*
DD (mg/L)	1.620 (0.970, 2.870)	1.460 (0.890, 2.175)	0.699
CK-MB (U/L)	0.480 (0.180, 0.770)	0.630 (0.360, 1.180)	0.072
WBC (10^3/ul)	14.770 (10.995, 22.225)	13.160 (11.290, 15.995)	0.052
LYM (10^3/ul)	2.660 (1.343, 3.330)	3.240 (2.465, 4.110)	0.035*
L%	16.150 (4.600, 27.175)	22.600 (13.450, 31.000)	0.181
GRAN (10^3/ul)	10.220 (7.105, 18.025)	8.320 (5.960, 11.530)	0.054
N%	67.500 (50.225, 80.500)	62.600 (42.200, 72.000)	0.080
MONO (10^3/ul)	0.600 (0.388, 0.838)	0.555 (0.418, 0.690)	0.356
Plt (10^3/ul)	337.000 (257.000, 392.000)	340.500 (293.500, 415.750)	0.731
RBC (10^6/ul)	4.070 (3.855, 4.310)	4.135 (3.903, 4.408)	0.264
Hct (%)	31.800 (30.075, 33.775)	33.350 (31.775, 35.050)	0.038*
Hb (g/L)	107.500 (102.25, 113.750)	111.500 (104.000, 117.000)	0.068
NLR (10^3/ul/10^3/ul)	4.344 (2.582, 7.481)	2.694 (1.725, 4.469)	0.006**
PLR (10^3/ul/10^3/ul)	144.595 (115.013, 185.782)	112.903 (83.460, 145.730)	0.007**
PCT (ng/mL)	0.495 (0.240, 2.830)	0.410 (0.210, 1.237)	0.320
CRP (mg/dl)	81.000 (52.000, 123.300)	41.490 (20.005, 71.890)	0.000***
ESR (mm/hour)	79.000 (76.000, 92.000)	64.000 (48.000, 83.000)	0.003**
IL-2 (pg/mL)	1.310 (1.010, 2.355)	0.830 (0.010, 2.940)	0.996
IL-10 (pg/mL)	5.690 (3.093, 12.328)	4.620 (3.580, 9.995)	0.709
IFN-γ (pg/mL)	1.250 (0.125, 2.200)	0.910 (0.075, 1.740)	0.574

Notes: *$p < 0.05$, **$p < 0.01$, ***$p < 0.001$.

Abbreviations: CALs, coronary artery lesions; NCALs, non-coronary artery lesions; PT, prothrombin time; APTT, activated partial thromboplastin time; Fbg, fibrinogen; TT, thrombin time; DD, D-dimer; CK-MB, creatine kinase-MB; WBC, white blood cell counts; LYM, lymphocyte count; L%, percentage of lymphocytes; GRAN, neutrophilic granulocyte count; N%, percentage of neutrophils; MONO, monocyte count; Plt, platelet counts; RBC, red blood cell counts; Hct, hematocrit; Hb, hemoglobin; NLR, neutrophil-to-lymphocyte ratio; PLR, platelet-to-lymphocyte ratio; PCT, procalcitonin; CRP, C-reactive protein, ESR, erythrocyte sedimentation rate; IL-2, interleukin-2; IL-10, interleukin-10; IFN-γ, interferon-gamma.

parameters: AUC, sensitivity, and specificity. Subsequent analysis revealed that the combination of Fbg and MFG-E8 resulted in an enhancement of the AUC value from 0.701 (95% confidence interval 0.618–0.775) to 0.943 (95% confidence interval 0.891–0.975), while the combination of TT and MFG-E8 yielded an increase of the AUC value from 0.701 (95% confidence interval 0.618–0.775) to 0.927 (95% confidence interval 0.871–0.964). Furthermore, the combined analysis of MFG-E8 with Fbg and TT not only raised the AUC value to 0.952 (95% confidence interval 0.902–0.981) but also achieved a sensitivity of 90.8% and a specificity of 92.31% (Figure 2 and Table 3).

Correlations Between MFG-E8 and Laboratory Parameters

As illustrated by the correlation heat map (Figure 3), the serum levels of MFG-E8 were negatively related to APTT, Fbg, WBC, N%, NLR, PLR, ESR, IL-2, IL-10, IFN-γ and positively related to TT, CK-MB, LYM, L% in the KD group.

Correlations Between MFG-E8 and Diameters of Coronary Artery

What can be clearly seen in Table 4 were the general associations of MFG-E8 with the four major coronary branches, not only in the direct measurements of internal diameter but also in the normalized Z-scores. Further analysis revealed that the correlations were concentrated in the CALs group and reflected by the left anterior descending branch (LAD) and the left circumflex branch (LCX).

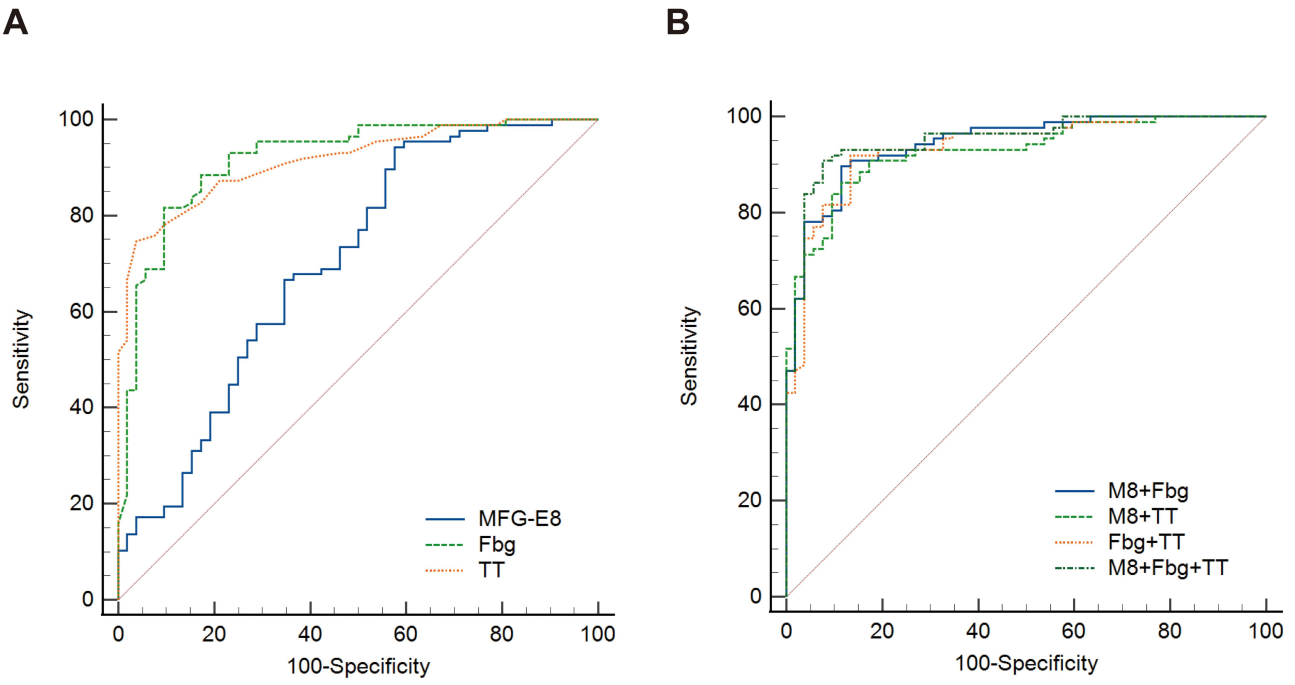

Figure 2 ROC curves of biomarkers to distinguish KD from FC. (**A**) Diagnostic performance of individual biomarkers. (**B**) Diagnostic performance of combined biomarkers. ROC, receiver operating characteristic.

MFG-E8 Expression in the Mouse Model

To confirm the role of MFG-E8 in the development of KD, we established a CAWS-induced murine model of KD vasculitis and examined the expression of MFG-E8 in it. As assessed by immunofluorescence, MFG-E8 was found to be localized around the coronary arteries in cardiac tissue and reached its peak expression on the 7th day after induction (Figure 4A). H&E staining at the indicated time points was performed to evaluate the grade of coronary arteritis, showing that the inflammatory cell infiltration peaked on the 14th day after induction (Figure 4B). Day 14 after CAWS induction was selected as the observation endpoint in this study. In line with clinical observations, serum MFG-E8 levels were significantly lower in the CAWS group (390.550 ± 97.114 ng/L) compared with the PBS group (615.857 ± 166.856 ng/L) at this time point ($p = 0.009$, Figure 4C). In contrast, consistent with fluorescence findings, MFG-E8 protein levels in cardiac tissue were significantly higher in the CAWS group compared with the PBS group ($p = 0.047$, Figure 4D).

MFG-E8 Alleviates CAWS-Induced KD-Like Vasculitis in Mice

Given the inconsistency between the expression of MFG-E8 protein and the severity of coronary artery inflammation in mice challenged with CAWS, we hypothesized that more MFG-E8 might be needed to ameliorate vasculitis. Weight loss,

Table 3 Predictive Ability of Biomarkers to Distinguish KD From FC

	AUC	95% CI	Cut-Off Value	Youden Index	Se (%)	Sp (%)	*p* value
MFG-E8	0.701	0.618–0.775	1113.313	0.366	94.32	42.31	<0.001***
Fbg	0.918	0.859–0.958	5.09	0.720	81.61	90.38	<0.001***
TT	0.915	0.856–0.956	15.3	0.709	74.71	96.15	<0.001***
MFG-E8+Fbg	0.943	0.891–0.975	0.562	0.781	89.66	88.46	<0.001***
MFG-E8+TT	0.927	0.871–0.964	0.660	0.747	86.21	88.46	<0.001***
Fbg+TT	0.934	0.880–0.969	0.514	0.785	91.95	86.54	<0.001***
MFG-E8+Fbg+TT	0.952	0.902–0.981	0.560	0.831	90.80	92.31	<0.001***

Notes: ***$p < 0.001$.

Abbreviations: FC, febrile controls; KD, Kawasaki disease; AUC, area under the curve; 95% CI, 95% confidence interval; Se, sensitivity; Sp, specificity; MFG-E8, Milk Fat Globule Epidermal Growth Factor 8; Fbg, fibrinogen; TT, thrombin time.

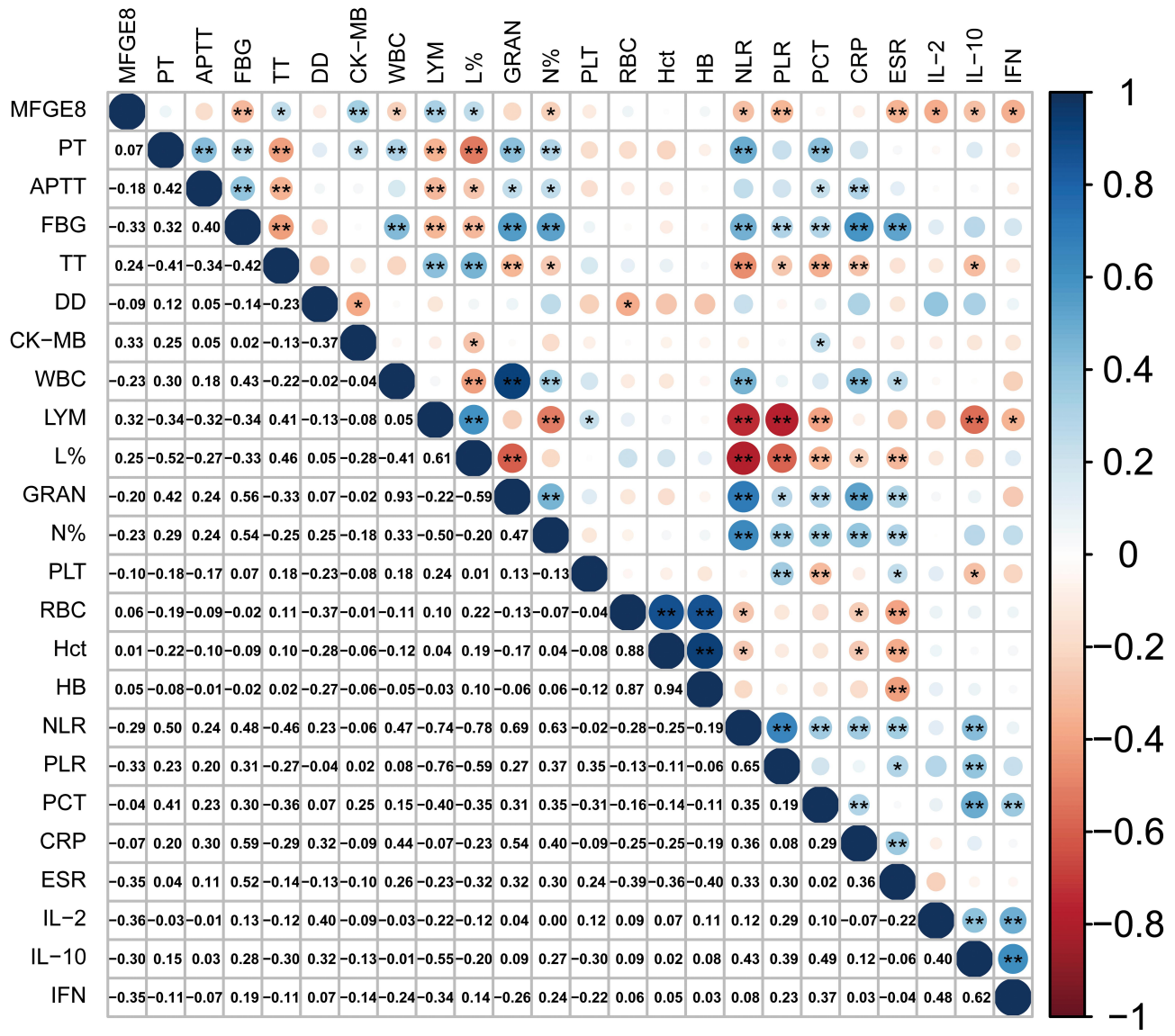

Figure 3 Correlation analysis between MFG-E8 and laboratory parameters for KD. Significance: *$p < 0.05$, **$p < 0.01$.
Abbreviations: PT, prothrombin time; APTT, activated partial thromboplastin time; Fbg, fibrinogen; TT, thrombin time; DD, D-dimer; CK-MB, creatine kinase-MB; WBC, white blood cell counts; LYM, lymphocyte count; L%, percentage of lymphocytes; GRAN, neutrophilic granulocyte count; N%, percentage of neutrophils; PLT, platelet counts; RBC, red blood cell counts; Hct, hematocrit; HB, hemoglobin; NLR, neutrophil-to-lymphocyte ratio; PLR, platelet-to-lymphocyte ratio; PCT, procalcitonin; CRP, C-reactive protein; ESR, erythrocyte sedimentation rate; IL-2, interleukin-2; IL-10, interleukin-10; IFN, interferon-gamma.

splenomegaly, expansion of the abdominal aorta, and inflammation of the aortic valve and coronary arteries were manifested in the CAWS-induced mouse model that resembles the typical vascular pathology of KD. MFG-E8 treatment apparently relieved weight loss (Figure 5A) and normalized the increased spleen length in the model mice (Figure 5B). When CAWS-induced vasculitis involved the abdominal aorta, some segments of the vessels were observed to increase in diameter which was significantly reduced after MFG-E8 administration (Figure 5C). H&E staining showed severe inflammatory cell infiltration around the aortic valve and coronary arteries ($p < 0.001$, Figure 5D), especially neutrophils ($p < 0.001$, Figure 5E), which was markedly attenuated with the MFG-E8 intervention ($p = 0.021$, Figure 5D; $p = 0.014$, Figure 5E).

MFG-E8 Alleviates Cardiac Pyroptosis in the Murine Model

Endothelial cell (EC) abnormalities are often regarded as the initiating step of vascular injury in KD. Vascular cell adhesion molecule-1 (VCAM-1), an essential molecule mediating the adhesion of many leukocytes to the vascular

https://doi.org/10.2147/JIR.S547634

Table 4 Correlations Between MFG-E8 Levels and Z-Value

	CALs (n=32)		NCALs (n=56)		KD (n=88)	
	r	*p*	*r*	*p*	*r*	*p*
LMCA	0.082	0.660	−0.153	0.261	−0.244	0.023*
LAD	−0.539	0.004**	−0.123	0.366	−0.361	0.001**
LCX	−0.406	0.024*	−0.074	0.593	−0.254	0.018*
RCA	−0.031	0.867	−0.117	0.390	−0.251	0.019*
z-value of LMCA	−0.144	0.457	−0.088	0.519	−0.230	0.034*
z-value of LAD	−0.504	0.007**	−0.101	0.448	−0.308	0.005**
z-value of LCX	−0.500	0.006**	−0.042	0.775	−0.251	0.027*
z-value of RCA	−0.013	0.946	−0.050	0.718	−0.226	0.037*

Notes: *$p < 0.05$, **$p < 0.01$.
Abbreviations: MFG-E8, Milk Fat Globule Epidermal Growth Factor 8; KD, Kawasaki disease; CALs, coronary artery lesions; NCALs, non-coronary artery lesions; LMCA, left main coronary artery; LAD, left anterior descending branch; LCX, left circumflex branch; RCA, right coronary artery.

endothelium and considered a marker of EC activation during inflammation, was detected to be expressed higher in the CAWS group than in the PBS group ($p < 0.0001$, Figure 6A). In contrast, MFG-E8 treatment reduced the expression of VCAM-1 ($p < 0.001$, Figure 6A), revealing a potential protective effect of MFG-E8 on ECs.

Pyroptosis is widely observed in inflammatory diseases, in which endothelial cell pyroptosis has been proven to be a critical pathophysiological event in KD, yet the role of MFG-E8 in this process is unclear. To verify the presence of pyroptosis in coronary endothelial cells, double-stained fluorescence was employed, with green fluorescence labeling CD31 and red fluorescence labeling NLRP3. As shown, the expression level of NLRP3 positioned in the endothelium was distinctly higher in the CAWS group than in the PBS group, which was decreased by MFG-E8 supplementation (Figure 6B). The following WB analysis presented consistent results that MFG-E8 treatment enabled a remarkable decrease in the levels of NLRP3 ($p = 0.001$), GSDMD-F ($p = 0.027$), and GSDMD-N ($p = 0.005$) proteins (Figure 6C), all of which were upregulated in the model group.

MFG-E8 Alleviates Oxidative Stress Levels in the Murine Model

Pyroptosis is an essential biological effect of oxidative stress. ROS can trigger the activation of NLRP3 inflammasome in endothelial cells upon external stimulation. Oxidative stress is known to be strongly enhanced during the acute phase of KD, in which the involvement of MFG-E8 has not been described. Thus, relevant markers, such as superoxide dismutase (SOD) and malondialdehyde (MDA), were examined in the serum of the mice. Compared to controls, low activity of SOD ($p = 0.006$) and high levels of MDA ($p < 0.0001$) were demonstrated in the model group (Figure 6D). MFG-E8 intervention eliminated these changes, reflecting its anti-oxidative stress activity in KD.

MFG-E8 Ameliorates KD-Treated EC Pyroptosis

The protective effect of MFG-E8 against coronary artery injury during the acute phase of KD has been demonstrated in the above experiments. To simulate the inflammatory environment of endothelial cells in vitro, we utilized KD serum-treated THP-1 cells co-cultured with EA.hy926 cells to create an in vitro system. Different concentrations of recombinant MFG-E8 protein were added before ECs in response to stimulation. The CCK-8 assay showed that the viability of EA.hy926 cells was decreased significantly by inflammatory exposure ($p < 0.001$, Figure 7A), which was rescued at 200 ng/mL of MFG-E8 ($p = 0.017$, Figure 7A). As a result, this concentration was selected for subsequent experiments. To confirm the phenomenon noted in the endothelium of coronary arteries in the murine model of vasculitis, transmission electron microscopy (TEM) was first used to observe the morphology of endothelial cells. As shown in Figure 7B, stimulated ECs showed larger and swelling mitochondria as well as blurring mitochondria cristae architecture. Besides, membrane rupture and pore formation were seen, suggesting inflammation-induced pyroptosis. Next, the cell membrane integrity was evaluated by lactate dehydrogenase (LDH) release assay, showing a markedly raised percentage of LDH

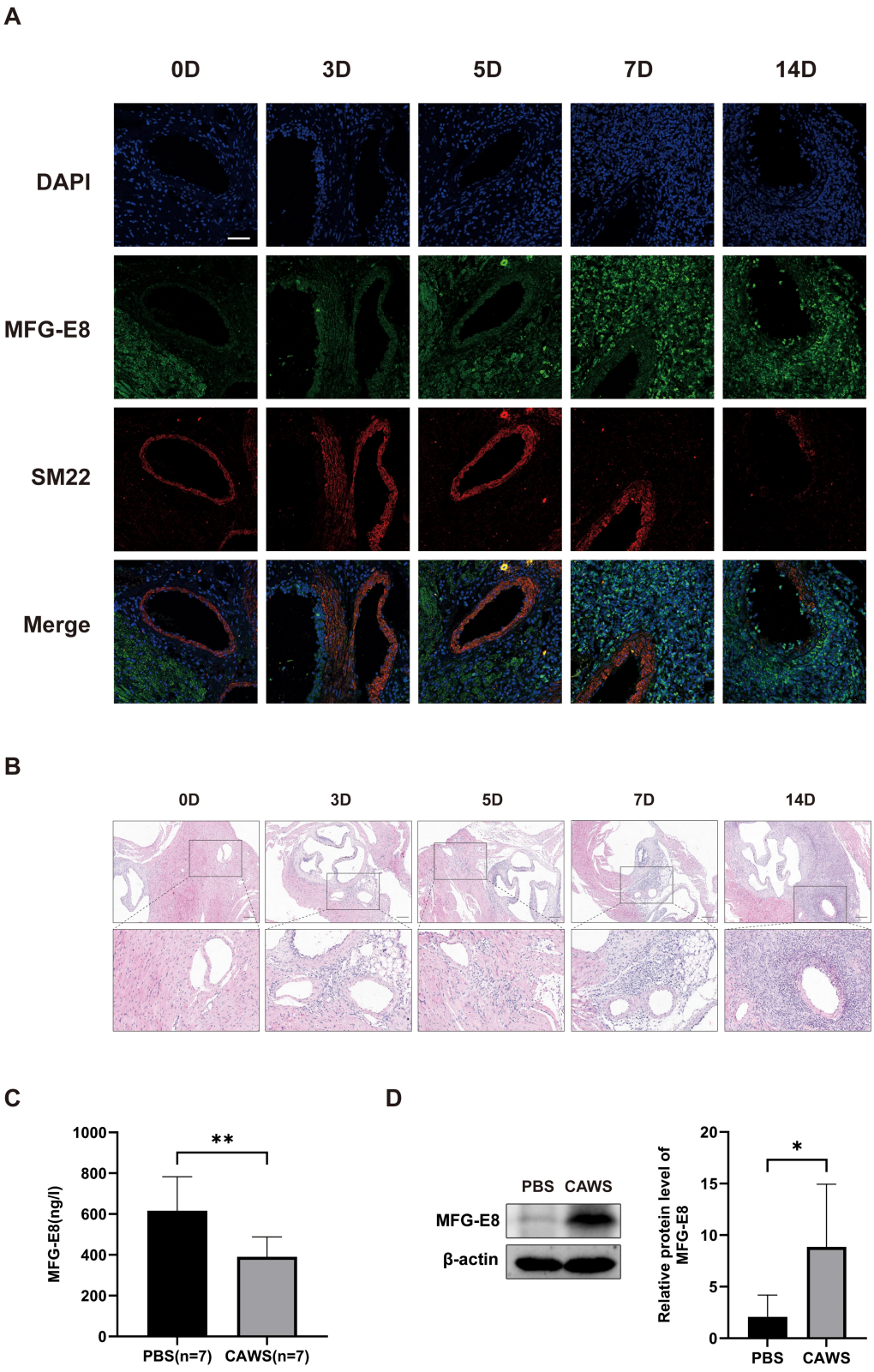

Figure 4 MFG-E8 expression in the mouse model. (**A**) MFG-E8 (green) expression at different time points (0D, 3D, 5D, 7D, 14D) post-CAWS injection was observed by immunofluorescence. SM22 (red) was used to locate the position of the coronary artery. Scale bar = 200μm, n=3. (**B**) Representative images from H&E staining at different time points post-CAWS injection. Scale bar = 200μm, n=3. (**C**) Serum MFG-E8 levels in the PBS group (n=7) and the CAWS group (n=7). Mice in the CAWS group were intraperitoneally injected daily with CAWS (4mg/body) dissolved in 0.2 mL of saline for 5 consecutive days, PBS group received an equal volume of saline injection. (**D**) WB strips and quantitative analysis (n=5) of MFG-E8 in heart tissues at 14-day post-CAWS injection. Significance: *$p < 0.05$, **$p < 0.01$.

https://doi.org/10.2147/JIR.S547634

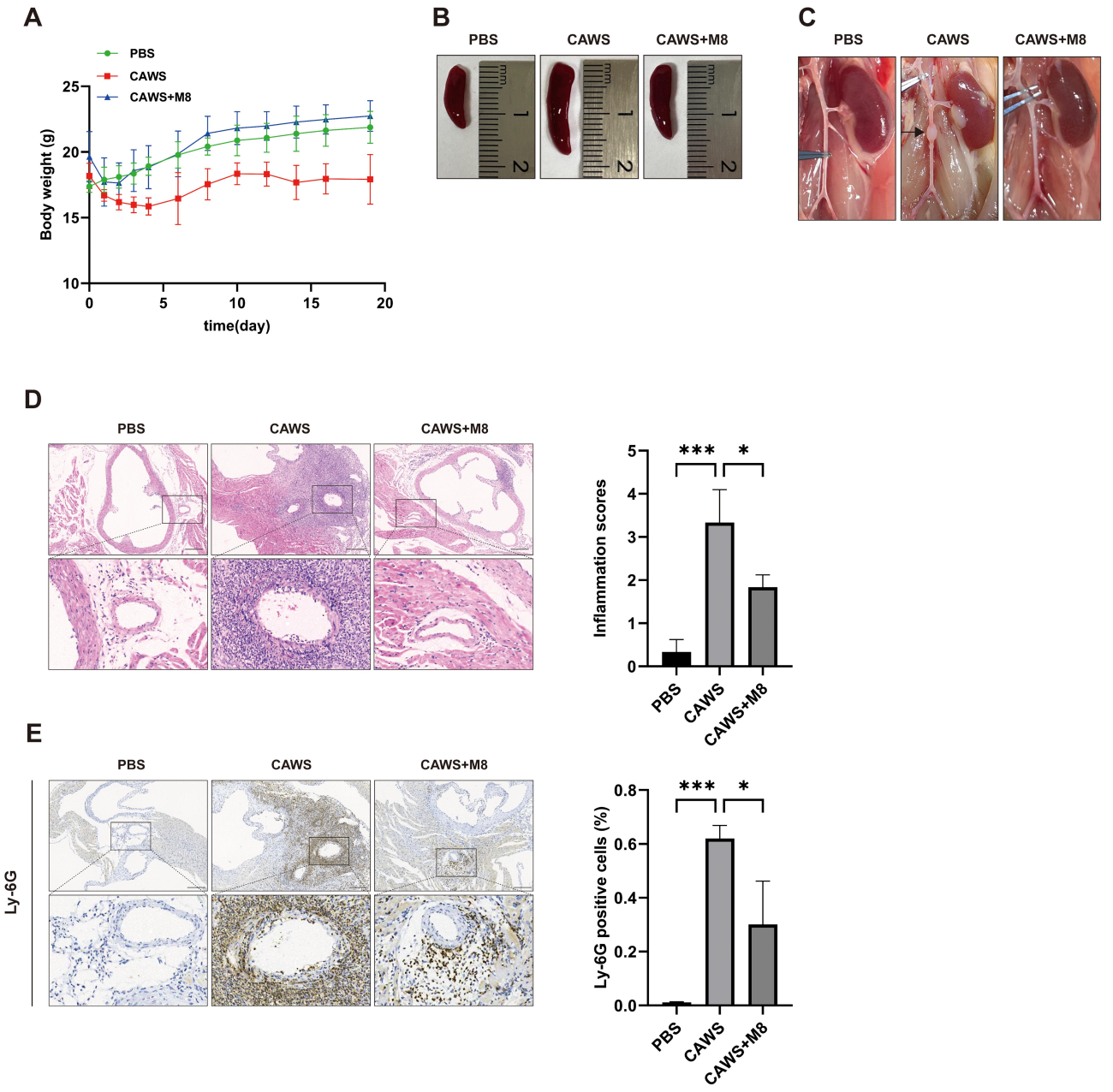

Figure 5 MFG-E8 alleviates CAWS-induced KD-like vasculitis in mice. PBS group: Served as the control; CAWS group: Served as the mo CAWS+M8 group: Received exogenous recombinant MFG-E8 protein during and after the CAWS induction. (**A**) Mean body weight change of mice in the three groups. n=5. (**B**) Representative images of the mice spleens on day 14. n=3. (**C**) Representative images of the abdominal aorta on day 14. n=3. The arrow indicates the abnormally dilated segment. (**D**) Representative H&E images of the aortic root and coronary arteries. Inflammation scores based on the comprehensive evaluation of inflammatory cell infiltration around the coronary arteries and the aortic root. Scale bar = 200μm, n=3. (**E**) Representative images of IHC staining for Ly-6G around the aortic valve and coronary arteries. Scale bar = 200μm, n=3. Significance: *$p < 0.05$, ***$p < 0.001$.

release in the model group ($p < 0.0001$, Figure 7C). MFG-E8 intervention ameliorated the morphological changes and reduced LDH release ($p < 0.0001$, Figure 7C). Moreover, the levels of pyroptosis-related proteins, including NLRP3 and GSDMD-N, were remarkably increased in KD serum-treated cells, which could be counteracted by MFG-E8 (Figure 7D). The above results revealed the beneficial effect of MFG-E8 on endothelial cell pyroptosis in the inflammatory environment of KD.

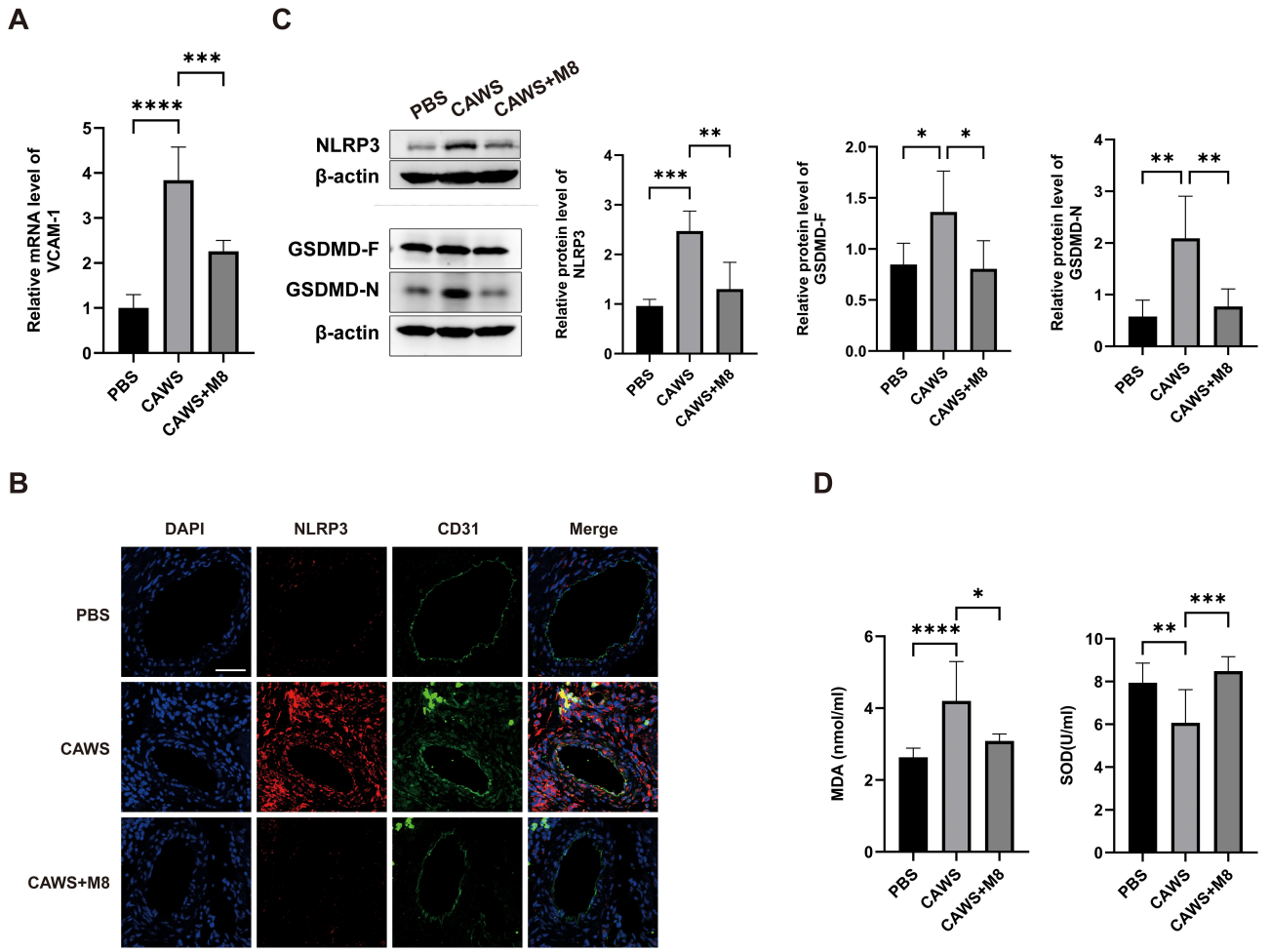

Figure 6 MFG-E8 alleviated cardiac pyroptosis and oxidative stress levels in a murine model of KD vasculitis. (**A**) The expression level of VCAM-1 in heart tissues (n=5). (**B**) NLRP3 expression levels were examined in the coronary artery endothelial cells by double staining of NLRP3 (red) and CD31 (green). Scale bar = 50μm, n=3. (**C**) WB strips and quantitative analysis of pyroptosis-related proteins in heart tissue. n=5. (**D**) The activity of SOD and the level of MDA in the serum of mice (n=8). Significance: *$p < 0.05$, **$p < 0.01$, ***$p < 0.001$; ****$p < 0.0001$.

MFG-E8 Ameliorates Oxidative Stress Imbalance in KD-Treated EC

Then, we examined the level of intracellular oxidative stress in ECs based on the above in vitro model. It was shown that MFG-E8 dramatically reduced the level of oxidative stress upon inflammation compared to the normal condition, as reflected by increased SOD ($p < 0.001$) and GSH-Px ($p = 0.026$) as well as decreased MDA ($p < 0.001$) (Figure 7E).

Discussion

MFG-E8, also known as lactadherin, is a secreted glycoprotein that was initially found as a bridging molecule between damaged or apoptotic cells and phagocytic cells. Given this clearance-mediated capacity, MFG-E8 has been considered to be an important regulator of the progression of many inflammatory and autoimmune diseases. Yet, the involvement of MFG-E8 in KD, an immune-related disease with systemic vasculitis as the main pathological change, is unclear. In the present study, the serum levels of MFG-E8 in the NC and FC groups were substantially higher than those in the KD group, especially in children complicated with CALs. Similar trends have also been reported in other diseases, such as rheumatoid arthritis,[29] ischemia/reperfusion injury, atherosclerosis,[30] sepsis,[31] etc., which are presumed to be influenced by the existence of inflammation or injury. Such low serum levels may result from two approaches. On the one hand, MFG-E8 could migrate toward damaged tissues in response to chemokines. When it is recruited around the coronary arteries, the target site of KD, the detectable level in the circulatory system will decrease correspondingly. On the other

https://doi.org/10.2147/JIR.S547634

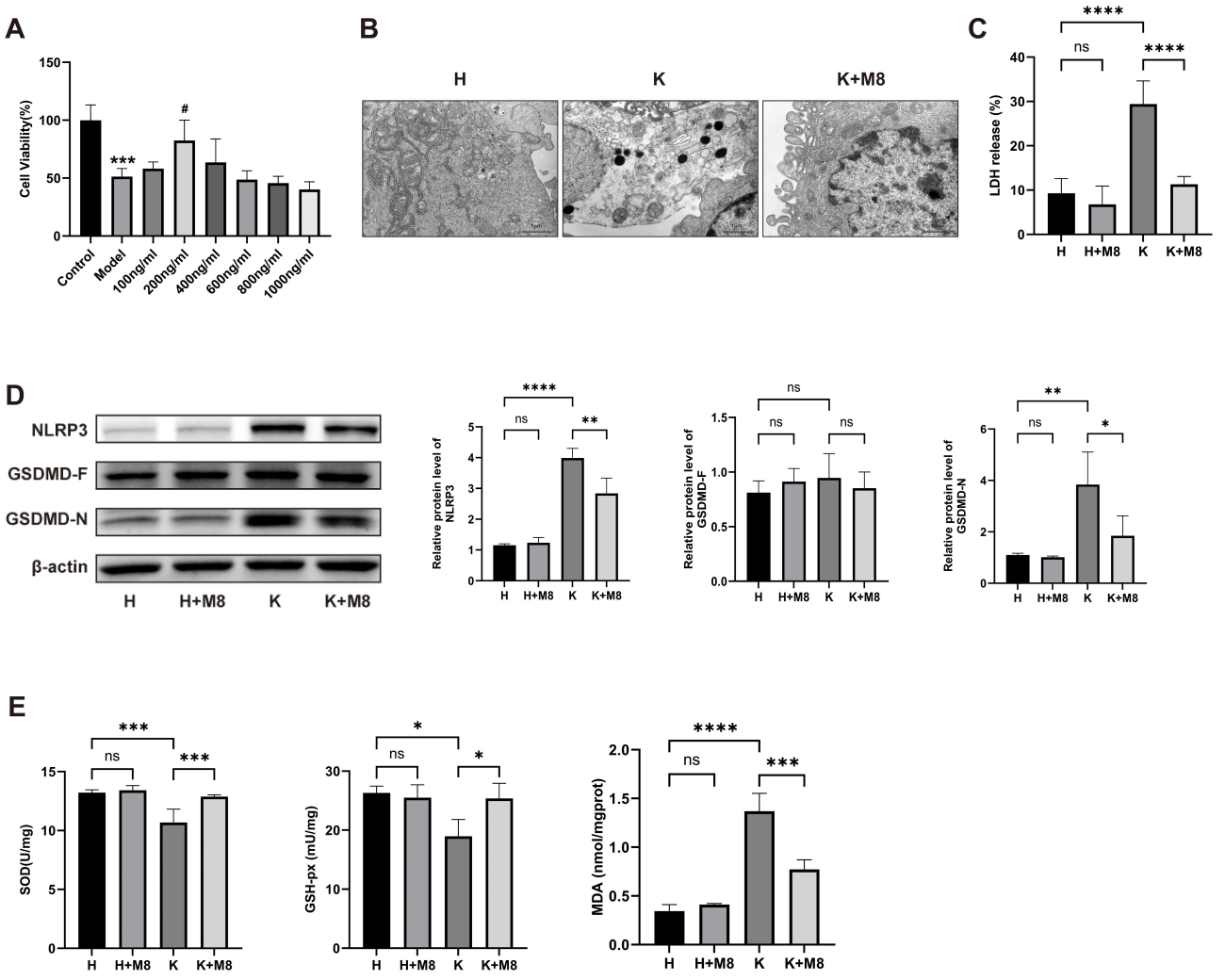

Figure 7 MFG-E8 improved KD-treated EC pyroptosis and oxidative stress. (**A**) EA.hy926 cells were cultured under normal (Control) or inflammation (Model) conditions with the indicated doses of MFG-E8 for 24 h, and cell viability was determined by CCK-8 assays. n=4. (**B**) Ultrathin EA.hy926 cell sections were scanned by TEM to assess mitochondrial and cell membrane damage. Scale bar = 1μm. (**C**) The LDH release in supernatants was expressed as the percentage of maximum. n=4. (**D**) WB strips and quantitative analysis of pyroptosis-related proteins in the treated endothelial cells. n=3. (**E**) The activity of SOD and GSH-px and the level of MDA in whole-cell lysates. n ≥ 3. Significance: ns, not significant; *$p < 0.05$, **$p < 0.01$, ***$p < 0.001$; ****$p < 0.0001$, $^{\#}p < 0.05$.

hand, as a common antigen that triggers KD, LPS has been found to negatively regulate the expression of MFG-E8 in macrophages,[32] resulting in a reduction of MFG-E8 released into the pouch.

In comparison with the FC group, significant changes in the KD group also included increased PT, APTT, Fbg, DD, WBC, GRAN, N%, NLR, PCT, and CRP, as well as decreased TT, CK-MB, L%, RBC, Hct, and Hb. We performed ROC analyses of the above indexes independently or in combination with MFG-E8. What is shown is that the two indexes, Fbg or TT, exhibited better performance in combined diagnosis when considering both the absolute value of AUC and the balance between sensitivity and specificity. Notably, a higher AUC value was obtained, accompanied by sensitivities and specificities over 90% when we applied these three indicators simultaneously for diagnosis. Hereby, it is reasonable to assume that MFG-E8 could provide valuable clues to distinguish the early stages of KD from other febrile illnesses in combination with other indicators.

Coronary artery lesions are the most concerning complication of KD and may lead to long-term cardiovascular sequelae, including myocardial infarction and sudden death. Currently, its incidence remains high. Although standardized IVIG treatment is considered effective, 5% of patients still fail to benefit from it.[33] Therefore, a better understanding of the mechanisms underlying CALs is needed to achieve more comprehensive treatment strategies.

In our study, MFG-E8 was expressed at lower levels in the CALs group compared to the NCALs group. A similar low expression was also found in LYM, Hct, and TT. In contrast, NLR, PLR, CRP, ESR, APTT, and Fbg were shown at a higher level. Interestingly, the majority of the above metrics that differed between groups were correlated with MFG-E8 in varying degrees. In general, MFG-E8 showed negative correlations with metrics that are usually recognized as indicative of inflammation, raising the possibility of its anti-inflammatory role in the acute phase of KD. Coherently with this hypothesis, MFG-E8 is equipped to exert anti-inflammatory effects through multiple pathways. For one thing, MFG-E8 restores the function of regulatory T lymphocytes suppressed by excessive accumulation of residual metabolites through promoting endocytosis of damaged cells.[34] Meanwhile, the NF-kB and MAPKs pathways in macrophages are inhibited upon receiving signals carried by MFG-E8, leading to a reduction in the release of downstream pro-inflammatory factors.[35] For another, MFG-E8 can directly bind to the integrin receptors αVβ3 or αVβ5 on the membrane surface independently of phagocytosis, activating the STAT3/SOCS3 pathway and thereby inhibiting the activation of NF-kB.[36] Additionally regulated is the TLR4 pathway that serves a major purpose in the amelioration of intestinal inflammation upon MFG-E8.[37] As an immune-related vasculitis, KD is characterized by a disruption of immune homeostasis, punctuated by a storm of uncontrolled inflammatory factors. The mechanisms mentioned above give MFG-E8 the opportunity to participate as a regulator in the progression of the acute phase of KD.

In terms of the approaches MFG-E8 takes to act on CALs, two dimensions are likely to be addressed. Foremost is its ability to defend against exogenous aggression. Cell loss is prevented through not only the multidirectional regulation of inflammatory pathways but also the diminution of oxidative stress levels.[38] Secondly, MFG-E8 possesses the property of repairing impaired tissues. The protein kinase C (PKC) pathway is activated by binding to PS on the cell surface, allowing the mucosa to be repaired and the tissue regenerated.[39] In addition, MFG-E8 exerts a critical effect on vascular endothelial growth factor (VEGF)-dependent neovascularisation, which is mediated by the phosphorylation of protein kinase B (Akt).[40]

Previous studies have shown that the left anterior descending branch (LAD) accounts for a large proportion of the distribution of CAA complicated by KD, especially in medium-sized aneurysms. In the present study, moderately negative correlations were found between MFG-E8 and the internal diameter of LAD as well as the normalized Z-scores, further revealing the significant position that MFG-E8 may hold in CALs secondary to Kawasaki disease.

In order to confirm the above assumption, we first established a CAWS-induced vasculitis model in mice. In contrast to the trend in serum, MFG-E8 in heart tissue mainly aggregated around coronary arteries and appeared alongside inflammatory cells at the initial time point. However, with further progression of inflammation, its expression instead declined. Considering the difference in the time points at which the two peaks appeared, we speculated that more MFG-E8 was required to perform beneficial functions at the foci during the acute phase of KD. Findings presented after supplementation of MFG-E8 corroborated our assumptions. Beyond the pathological features mimicking the phenotype of coronary artery lesions in the clinic, dilatation of the abdominal aorta formed following inflammation can also be observed in the murine model used for this study. While the high incidence of this manifestation was detected on day 28 after CAWS induction, it was also seen sparingly on day 14, the endpoint of this study. MFG-E8 treatment effectively reduced its occurrence. Besides, an improvement in splenomegaly was also described. Neutrophils have been reported to be activated by cytokines and subsequently mediate damage to vascular endothelial and smooth muscle cells, suggesting its substantial involvement in the pathological processes of coronary arterial injury at the early stage of KD.[41,42] Consistently, extensive neutrophil infiltration has been observed in the CAWS-induced vasculitis model, whereas administration of neutrophil-neutralizing antibodies effectively alleviates inflammation, emphasizing its important role in this process.[43] Accordingly, we evaluated coronary artery inflammation by integrating inflammation scores from H&E staining with the percentage of neutrophils obtained from immunohistochemical analysis, confirming the beneficial effect of MFG-E8. The observed reduction in neutrophil infiltration may be due to MFG-E8's ability to suppress neutrophil migration towards chemokines[44] or inhibit their adhesion to endothelial cells.[45] Thus, we have reason to believe that MFG-E8 is likely to provide a beneficial effect in the development of vasculitis during the acute phase of KD, although the specific aspects of this impact remain unclear.

Pyroptosis is a mode of programmed cell death characterized by heightened inflammation, which is widely involved in the occurrence and progression of various diseases and is increasingly prominent in the cardiovascular field. Endothelial cell pyroptosis has been proposed to play an essential role in coronary artery lesions during the acute phase of KD. MFG-E8, a secreted glycoprotein, has been reported to be effective in alleviating intervertebral disc degeneration,[46] improving the

inflammatory microenvironment of the kidney,[47] and promoting wound healing in diabetes[48] by inhibiting the activation of NLRP3 inflammasome. Hence, we chose endothelial cell pyroptosis as an entry point for our research.

It was observed that the significantly elevated level of cardiac pyroptosis in the model group tended to be normal upon MFG-E8 administration. Further localization analyses exhibited the same trend in the levels of NLRP3 inflammasome expressed in the endothelium, pointing to a counteracting action against endothelial cell pyroptosis. Meanwhile, an in vitro model of serum-treated THP-1 co-cultured with endothelial cells was utilized to validate the phenotype involved in mice, where consistent results were obtained. Accordingly, we can consider that MFG-E8 possesses the ability to alleviate the pyroptosis of coronary endothelial cells in the acute phase of KD.

Endoplasmic reticulum stress, as an upstream trigger of pyroptosis,[49] has been reported to actively participate in the inflammatory progression during the acute phase of KD.[50] Vascular endothelial cells, in particular, are sensitively responsive to this stimulus due to the abundant endoplasmic reticulum structures within them. Research has revealed that MFG-E8 could exert a protective effect against pancreatitis by inhibiting endoplasmic reticulum stress and maintaining cellular homeostasis, in terms of not only attenuating the damage of alveolar cells in the acute phase[51] but also mitigating the progression of fibrosis in the chronic phase.[52] To determine whether MFG-E8 is involved in oxidative stress during the acute phase of KD, relevant biomarkers were assayed in vivo and in vitro. As a result, MFG-E8 was shown to be effective in improving the imbalanced redox state in the model group, both at the level of the heart as a whole and specifically in vascular endothelial cells.

Although the interaction between oxidative stress and pyroptosis in the cardiovascular field has been adequately documented to date, it remains unclear whether MFG-E8 can alleviate endothelial pyroptosis through oxidative stress pathways, thereby providing beneficial effects on vascular inflammation during the acute phase of KD. Thus, some experiments on this concept need to be accomplished in the future to better elucidate the specific mechanisms by which MFG-E8 performs its protective functions in KD.

Limitations of This Study

The present study has observed the effects of MFG-E8 on the endothelium in a manner of exogenous administration. Nevertheless, in light of the immunomodulatory capabilities of MFG-E8 and the background of multiple immune participation in KD, it seems necessary to carry out studies where MFG-E8 indirectly acts on endothelial cells. Alternatively, to obtain results about the direct action of MFG-E8, constructing a conditional knockout mouse model for its integrin receptors in vascular endothelial cells would be a better choice. In addition, morphological changes have often already occurred when coronary artery lesions could be clinically detected. Consequently, studies targeting smooth muscle cells could provide a more comprehensive theoretical foundation for the clinical application of MFG-E8.

Conclusions

This study proposes that MFG-E8, in combination with other indicators, may assist in distinguishing Kawasaki disease KD from other febrile diseases at an early stage. Furthermore, clinical analyses revealed a correlation between MFG-E8 and coronary artery lesions. Validation in both a murine coronary arteritis model and an endothelial inflammation model confirmed the protective role of MFG-E8, involving attenuation of endothelial pyroptosis and oxidative stress. In summary, these findings not only position MFG-E8 as a tool for the early differential diagnosis of KD, but also provide a theoretical basis for considering it as a potential therapeutic target for coronary artery injury.

Abbreviations

PT, prothrombin time; APTT, activated partial thromboplastin time; Fbg, fibrinogen; TT, thrombin time; DD, D-dimer; CK-MB, creatine kinase-MB; WBC, white blood cell counts; LYM, lymphocyte count; L%, percentage of lymphocytes; GRAN, neutrophilic granulocyte count; N%, percentage of neutrophils; Plt, platelet counts; RBC, red blood cell counts; Hct, hematocrit; HB, hemoglobin; NLR, neutrophil-to-lymphocyte ratio; PLR, platelet-to-lymphocyte ratio; PCT, procalcitonin; CRP, C-reactive protein; ESR, erythrocyte sedimentation rate; IL-2, interleukin-2; IL-10, interleukin-10; IFN-γ, interferon-gamma; KD, Kawasaki disease; NC, normal controls; FC, febrile controls; CALs, coronary artery lesions; CAA, coronary artery aneurysms; ROC, receiver operating characteristic; MFG-E8, Milk Fat Globule Epidermal

Growth Factor 8; IVIG, intravenous immunoglobulin; NLRP3, NOD-like receptor thermal protein domain associated protein 3; CAWS, Candida albicans cell wall extracts; VCAM-1, vascular cell adhesion molecule-1; H&E, Hematoxylin and eosin; IHC, immunohistochemistry; WB, Western Blot; SOD, superoxide dismutase; GSH-px, glutathione peroxidase; MDA, malondialdehyde.

Ethics Approval and Informed Consent

The study was approved by the Ethics Committee of the Children's Hospital of Chongqing Medical University and was conducted in accordance with the Declaration of Helsinki. Informed consent was obtained from all parents or participants included in the study.

Data Sharing Statement

The data supporting the findings of this study are available from the corresponding author upon reasonable request.

Acknowledgments

The authors thank the Institute of Pediatrics, Children's Hospital, affiliated to Chongqing Medical University, for providing the experimental platform.

Author Contributions

All authors made a significant contribution to the work reported, whether that is in the conception, study design, execution, acquisition of data, analysis and interpretation, or in all these areas; took part in drafting, revising or critically reviewing the article; gave final approval of the version to be published; have agreed on the journal to which the article has been submitted; and agree to be accountable for all aspects of the work.

Funding

The grant from the National Clinical Research Center for Child Health and Disorders (No. NCRCCHD-2020-GP-02) and the Chongqing Post-graduate Research Innovation Project (No. CYB20159).

Disclosure

The authors report no conflicts of interest in this work.

References

1. Nakamura Y. Kawasaki disease: epidemiology and the lessons from it. *Int J Rheum Dis*. 2018;21(1):16–19. doi:10.1111/1756-185X.13211
2. Shulman ST, Rowley AH. Kawasaki disease: insights into pathogenesis and approaches to treatment. *Nat Rev Rheumatol*. 2015;11(8):475–482. doi:10.1038/nrrheum.2015.54
3. Hata A, Onouchi Y. Susceptibility genes for Kawasaki disease: toward implementation of personalized medicine. *J Hum Genet*. 2009;54(2):67–73. doi:10.1038/jhg.2008.9
4. Wu MH, Chen HC, Yeh SJ, et al. Prevalence and the long-term coronary risks of patients with Kawasaki disease in a general population <40 years: a national database study. *Circ Cardiovasc Qual Outcomes*. 2012;5(4):566–570. doi:10.1161/CIRCOUTCOMES.112.965194
5. Kato H, Sugimura T, Akagi T, et al. Long-term consequences of Kawasaki disease. A 10- to 21-year follow-up study of 594 patients. *Circulation*. 1996;94(6):1379–1385. doi:10.1161/01.CIR.94.6.1379
6. Newburger JW, Takahashi M, Gerber MA, et al. Diagnosis, treatment, and long-term management of Kawasaki disease: a statement for health professionals from the Committee on Rheumatic Fever, Endocarditis, and Kawasaki Disease, Council on Cardiovascular Disease in the Young. *Am Heart Assoc Pediatrics*. 2004;114(6):1708–1733.
7. Furusho K, Kamiya T, Nakano H, et al. High-dose intravenous gammaglobulin for Kawasaki disease. *Lancet*. 1984;2(8411):1055–1058. doi:10.1016/S0140-6736(84)91504-6
8. Yoshikane Y, Okuma Y, Miyamoto T, et al. Serum tenascin-C predicts resistance to steroid combination therapy in high-risk Kawasaki disease: a multicenter prospective cohort study. *Pediatr Rheumatol Online J*. 2021;19(1):82. doi:10.1186/s12969-021-00562-w
9. Hao S, Jin B, Tan Z, et al. A classification tool for differentiation of Kawasaki disease from other febrile illnesses. *J Pediatr*. 2016;176:114–120e118. doi:10.1016/j.jpeds.2016.05.060
10. Han RK, Sinclair B, Newman A, et al. Recognition and management of Kawasaki disease. *CMAJ*. 2000;162(6):807–812.
11. Takahashi K, Oharaseki T, Yokouchi Y. Update on etio and immunopathogenesis of Kawasaki disease. *Curr Opin Rheumatol*. 2014;26(1):31–36. doi:10.1097/BOR.0000000000000010
12. Hicar MD. Antibodies and immunity during Kawasaki disease. *Front Cardiovasc Med*. 2020;7:94. doi:10.3389/fcvm.2020.00094

13. Eleftheriou D, Levin M, Shingadia D, et al. Management of Kawasaki disease. *Arch Dis Child*. 2014;99(1):74–83. doi:10.1136/archdischild-2012-302841
14. Wallace CA, French JW, Kahn SJ, et al. Initial intravenous gammaglobulin treatment failure in Kawasaki disease. *Pediatrics*. 2000;105(6):E78. doi:10.1542/peds.105.6.e78
15. McCrindle BW, Rowley AH, Newburger JW, et al. Diagnosis, treatment, and long-term management of Kawasaki disease: a scientific statement for health professionals from the American Heart Association. *Circulation*. 2017;135(17):e927–e999. doi:10.1161/CIR.0000000000000484
16. Yu P, Zhang X, Liu N, et al. Pyroptosis: mechanisms and diseases. *Signal Transduct Target Ther*. 2021;6(1):128. doi:10.1038/s41392-021-00507-5
17. Toldo S, Abbate A. The role of the NLRP3 inflammasome and pyroptosis in cardiovascular diseases. *Nat Rev Cardiol*. 2024;21(4):219–237. doi:10.1038/s41569-023-00946-3
18. Shahi A, Afzali S, Firoozi Z, et al. Potential roles of NLRP3 inflammasome in the pathogenesis of Kawasaki disease. *J Cell Physiol*. 2023;238 (3):513–532. doi:10.1002/jcp.30948
19. Takahashi M. NLRP3 inflammasome as a key driver of vascular disease. *Cardiovasc Res*. 2022;118(2):372–385. doi:10.1093/cvr/cvab010
20. Jia C, Zhang J, Chen H, et al. Endothelial cell pyroptosis plays an important role in Kawasaki disease via HMGB1/RAGE/cathespin B signaling pathway and NLRP3 inflammasome activation. *Cell Death Dis*. 2019;10(10):778. doi:10.1038/s41419-019-2021-3
21. Aziz M, Jacob A, Matsuda A, et al. Review: milk fat globule-EGF factor 8 expression, function and plausible signal transduction in resolving inflammation. *Apoptosis*. 2011;16(11):1077–1086. doi:10.1007/s10495-011-0630-0
22. Yi YS. Functional role of milk fat globule-epidermal growth factor VIII in macrophage-mediated inflammatory responses and inflammatory/autoimmune diseases. *Mediators Inflamm*. 2016;2016:5628486. doi:10.1155/2016/5628486
23. Chiang HY, Chu PH, Chen SC, et al. MFG-E8 regulates vascular smooth muscle cell migration through dose-dependent mediation of actin polymerization. *J Am Heart Assoc*. 2021;10(11):e020870. doi:10.1161/JAHA.121.020870
24. Chiang HY, Chu PH, Lee TH. MFG-E8 mediates arterial aging by promoting the proinflammatory phenotype of vascular smooth muscle cells. *J Biomed Sci*. 2019;26(1):61. doi:10.1186/s12929-019-0559-0
25. Wang B, Ge Z, Wu Y, et al. MFGE8 is down-regulated in cardiac fibrosis and attenuates endothelial-mesenchymal transition through Smad2/3-Snail signalling pathway. *J Cell Mol Med*. 2020;24(21):12799–12812. doi:10.1111/jcmm.15871
26. Howangyin KY, Zlatanova I, Pinto C, et al. Myeloid-epithelial-reproductive receptor tyrosine kinase and milk fat globule epidermal growth factor 8 coordinately improve remodeling after myocardial infarction via local delivery of vascular endothelial growth factor. *Circulation*. 2016;133 (9):826–839. doi:10.1161/CIRCULATIONAHA.115.020857
27. Tada R, Nagi-Miura N, Adachi Y, et al. The influence of culture conditions on vasculitis and anaphylactoid shock induced by fungal pathogen Candida albicans cell wall extract in mice. *Microb Pathog*. 2008;44(5):379–388. doi:10.1016/j.micpath.2007.10.013
28. Stock AT, Hansen JA, Sleeman MA, et al. GM-CSF primes cardiac inflammation in a mouse model of Kawasaki disease. *J Exp Med*. 2016;213 (10):1983–1998. doi:10.1084/jem.20151853
29. Albus E, Sinningen K, Winzer M, et al. Milk Fat Globule-Epidermal Growth Factor 8 (MFG-E8) is a novel anti-inflammatory factor in rheumatoid arthritis in mice and humans. *J Bone Miner Res*. 2016;31(3):596–605. doi:10.1002/jbmr.2721
30. Ait-Oufella H, Kinugawa K, Zoll J, et al. Lactadherin deficiency leads to apoptotic cell accumulation and accelerated atherosclerosis in mice. *Circulation*. 2007;115(16):2168–2177. doi:10.1161/CIRCULATIONAHA.106.662080
31. Matsuda A, Jacob A, Wu R, et al. Milk fat globule-EGF factor VIII in sepsis and ischemia-reperfusion injury. *Mol Med*. 2011;17(1–2):126–133. doi:10.2119/molmed.2010.00135
32. Miksa M, Amin D, Wu R, et al. Fractalkine-induced MFG-E8 leads to enhanced apoptotic cell clearance by macrophages. *Mol Med*. 2007;13 (11–12):553–560. doi:10.2119/2007-00019.Miksa
33. Galeotti C, Bayry J, Kone-Paut I, et al. Kawasaki disease: aetiopathogenesis and therapeutic utility of intravenous immunoglobulin. *Autoimmun Rev*. 2010;9(6):441–448. doi:10.1016/j.autrev.2009.12.004
34. Tan Y, Alkhamees B, Jia D, et al. MFG-E8 is critical for embryonic stem cell-mediated T cell immunomodulation. *Stem Cell Reports*. 2015;5 (5):741–752. doi:10.1016/j.stemcr.2015.09.005
35. Miksa M, Wu R, Dong W, et al. Immature dendritic cell-derived exosomes rescue septic animals via milk fat globule epidermal growth factor-factor VIII [corrected]. *J Immunol*. 2009;183(9):5983–5990. doi:10.4049/jimmunol.0802994
36. Aziz M, Jacob A, Matsuda A, et al. Pre-treatment of recombinant mouse MFG-E8 downregulates LPS-induced TNF-alpha production in macrophages via STAT3-mediated SOCS3 activation. *PLoS One*. 2011;6(11):e27685. doi:10.1371/journal.pone.0027685
37. Aziz MM, Ishihara S, Mishima Y, et al. MFG-E8 attenuates intestinal inflammation in murine experimental colitis by modulating osteopontin-dependent alphavbeta3 integrin signaling. *J Immunol*. 2009;182(11):7222–7232. doi:10.4049/jimmunol.0803711
38. Cui Y, Luo L, Zeng Z, et al. MFG-E8 stabilized by deubiquitinase USP14 suppresses cigarette smoke-induced ferroptosis in bronchial epithelial cells. *Cell Death Dis*. 2023;14(1):2. doi:10.1038/s41419-022-05455-8
39. Bu HF, Zuo XL, Wang X, et al. Milk fat globule-EGF factor 8/lactadherin plays a crucial role in maintenance and repair of murine intestinal epithelium. *J Clin Invest*. 2007;117(12):3673–3683. doi:10.1172/JCI31841
40. Silvestre JS, Thery C, Hamard G, et al. Lactadherin promotes VEGF-dependent neovascularization. *Nat Med*. 2005;11(5):499–506. doi:10.1038/nm1233
41. Takahashi K, Oharaseki T, Naoe S, et al. Neutrophilic involvement in the damage to coronary arteries in acute stage of Kawasaki disease. *Pediatr Int*. 2005;47(3):305–310. doi:10.1111/j.1442-200x.2005.02049.x
42. Huang J, Wu S, Cao S, et al. Neutrophil-derived semaphorin 4D induces inflammatory cytokine production of endothelial cells via different plexin receptors in Kawasaki Disease. *Biomed Res Int*. 2020;2020:6663291. doi:10.1155/2020/6663291
43. Miyabe C, Miyabe Y, Miura NN, et al. Am80, a retinoic acid receptor agonist, ameliorates murine vasculitis through the suppression of neutrophil migration and activation. *Arthritis Rheum*. 2013;65(2):503–512. doi:10.1002/art.37784
44. Aziz M, Yang WL, Corbo LM, et al. MFG-E8 inhibits neutrophil migration through alphavbeta(3)-integrin-dependent MAP kinase activation. *Int J Mol Med*. 2015;36(1):18–28. doi:10.3892/ijmm.2015.2196
45. Hirano Y, Yang WL, Aziz M, et al. MFG-E8-derived peptide attenuates adhesion and migration of immune cells to endothelial cells. *J Leukoc Biol*. 2017;101(5):1201–1209. doi:10.1189/jlb.3A0416-184RR
46. Ma H, Xie C, Chen Z, et al. MFG-E8 alleviates intervertebral disc degeneration by suppressing pyroptosis and extracellular matrix degradation in nucleus pulposus cells via Nrf2/TXNIP/NLRP3 axis. *Cell Death Discov*. 2022;8(1):209. doi:10.1038/s41420-022-01002-8

47. Brissette MJ, Laplante P, Qi S, et al. Milk fat globule epidermal growth factor-8 limits tissue damage through inflammasome modulation during renal injury. *J Leukoc Biol*. 2016;100(5):1135–1146. doi:10.1189/jlb.3A0515-213RR
48. Huang W, Jiao J, Liu J, et al. MFG-E8 accelerates wound healing in diabetes by regulating "NLRP3 inflammasome-neutrophil extracellular traps" axis. *Cell Death Discov*. 2020;6:84. doi:10.1038/s41420-020-00318-7
49. Zheng D, Liu J, Piao H, et al. ROS-triggered endothelial cell death mechanisms: focus on pyroptosis, parthanatos, and ferroptosis. *Front Immunol*. 2022;13:1039241. doi:10.3389/fimmu.2022.1039241
50. Tsuge M, Uda K, Eitoku T, et al. Roles of oxidative injury and nitric oxide system derangements in Kawasaki disease pathogenesis: a systematic review. *Int J Mol Sci*. 2023;24(20). doi:10.3390/ijms242015450
51. Ren Y, Liu W, Zhang J, et al. MFG-E8 maintains cellular homeostasis by suppressing endoplasmic reticulum stress in pancreatic exocrine acinar cells. *Front Cell Dev Biol*. 2021;9:803876. doi:10.3389/fcell.2021.803876
52. Ren Y, Cui Q, Zhang J, et al. Milk fat globule-EGF factor 8 alleviates pancreatic fibrosis by inhibiting ER stress-induced chaperone-mediated autophagy in mice. *Front Pharmacol*. 2021;12:707259. doi:10.3389/fphar.2021.707259